Chapter 3

Elastic scattering and comparison of reaction cross section with fusion-fission cross section of the ^{6,7}Li + ^{232}Th systems

3.1 Introduction

The study of nuclear reactions that involve weakly bound nuclei shows different characteristics in the energy dependence of the optical potential parameters. In this phenomena the nuclei at energies near the Coulomb barrier, the real part shows a characteristic localized peak and imaginary part decreases as the bombarding energy decreases towards the Coulomb barrier, known as Threshold Anomaly (TA) [1, 13, 31, 62]. Nowadays, the measurement and analysis of elastic scattering angular distribution have been establish for the study of breakup phenomena. If any reaction or channel pairing effects are present then the result obtained may be used to observe the presence of threshold or breakup threshold anomaly through the study of energy dependence optical potential parameters [38]. However, in the observation of breakup threshold anomaly in some cases of target masses ranging from light to heavy mass nuclei does not hold good rather it shows absence of TA. This means no specific observation of characteristics exist that shows presence of TA/BTA. Thus, the study of threshold and breakup threshold anomaly in case of weakly bound nuclei on different target is important, at

below and around the Coulomb barrier. This is due to the fact that there is a coupling of elastic and direct reaction channels, giving rise to attractive real dynamic polarization potential. As a result, there is an enhancement of fusion reaction cross section due to the decrease in the Coulomb barrier.

3.1.1 Present work

In this thesis, we have carried out the study of threshold and breakup threshold anomaly, from the measurements of elastic scattering using ^{6,7}Li projectiles on a heavy mass target, ^{232}Th. The measurement of the elastic scattering have been carried out for ^{6,7}Li + ^{232}Th reactions at different energies. The Coulomb barrier for ^{6,7}Li + ^{232}Th systems is approximately 32 MeV. For the study of elastic scattering angular distribution we have taken 25% below and 40% above the Coulomb barrier energy. For the weakly bound projectile, in order to understand the breakup reactions, the total reaction cross section are also studied around the Coulomb barrier energies.

There have been renewed interest in elastic scattering studies using weakly bound projectiles, with the observation of the rapid variation of the optical potential parameters with energy around the Coulomb barrier. Thus the investigation of TA/ BTA has been one of the mode to check the impact of the breakup reaction and different reaction channels on the elastic scattering and fusion reaction [63]. In the study of elastic scattering angular distribution on various medium and heavy mass targets like ^{59}Co, ^{138}Ba, ^{208}Pb, ^{80}Se [14, 15, 16, 5] the TA/BTA was obtained. According to the studies of above systems the enhancement in the real potential near the Coulomb barrier energies, shows the presence of threshold anomaly.

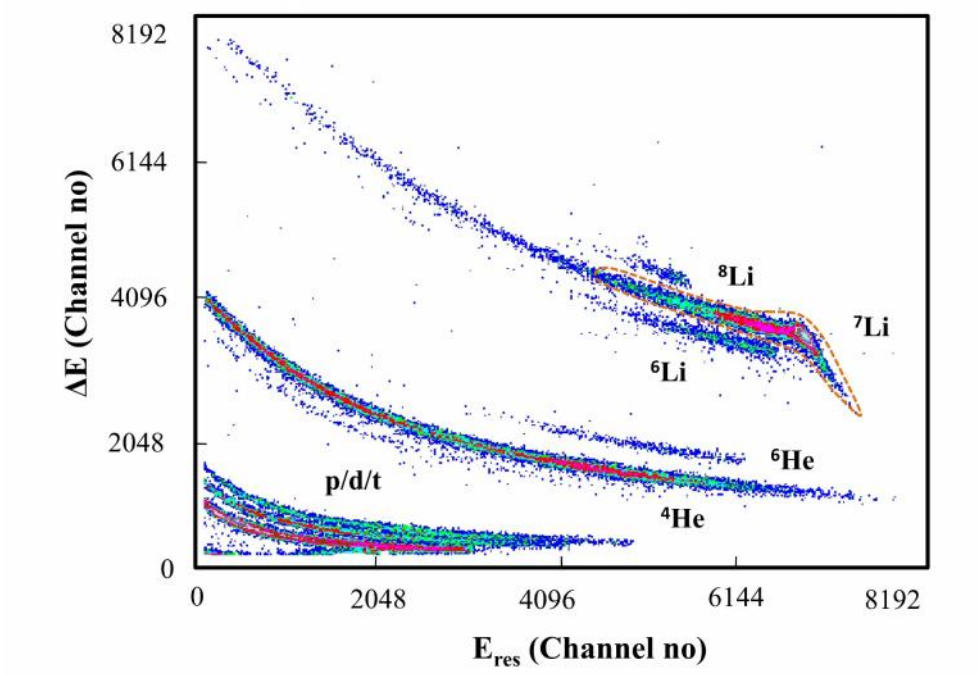

Figure 3.1: A 2D spectrum (Δ E vs E_{res}) for the ^{7}Li + ^{232}Th system at E_{lab} = 44 MeV and $\theta_{lab} = 60^{o}$.

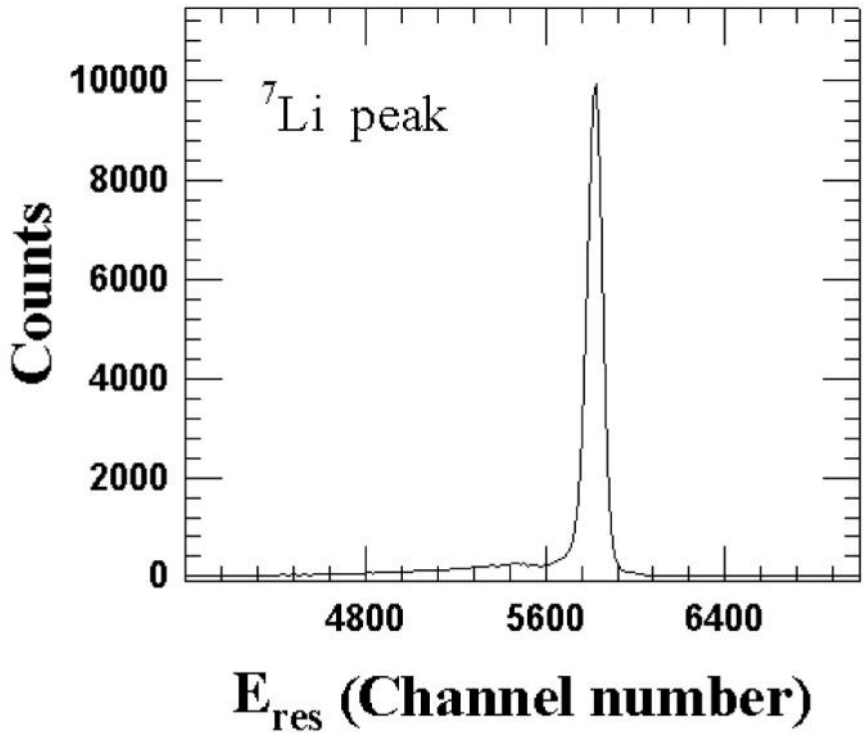

Figure 3.2: The projection of the ^{7}Li elastic peak of the bi-parametric ΔE vs E_{res} spectrum (from above two dimensional fig.(3.1)).

The breakup threshold energy of ^{6}Li (α + d) nuclei is 1.48 MeV. For ^{7}Li (α + t) the breakup threshold energy is 2.47 MeV. This phenomenon of TA is not satisfactorily understood in the case of ^{6}Li projectile. In other phenomena, know as breakup threshold anomaly (BTA), being observed mostly in weakly bound nuclei. For the study of elastic scattering angular distribution of ^{6}Li projectile, large number of papers are available on different targets like ^{27}Al, ^{64}Ni, ^{64}Zn, ^{90}Zr, ^{138}Ba, ^{144}Sm, ^{208}Pb, ^{209}Bi, ^{116,112}Sn, and ^{80}Se [5, 15, 16, 4, 22, 23, 24, 25, 27, 26] has been published and presented the result in term of breakup threshold anomaly. According to the study of above systems small enhancement in the imaginary part of the potential around the Coulomb barrier, may be called as absence of normal TA. The results show contradictory conclusions on TA/BTA. Therefore, more measurements involving weakly bound projectiles with different targets are required to understand the systematic of TA and BTA behavior for the potential describing the elastic scattering, which can be called as absence of normal TA. The earlier measurements to study TA/BTA using weakly bound projectiles on different target nuclei show several contradictory results and conclusions. Therefore, there is a strong reason to re-investigate and understand the phenomena of TA/BTA using the measurements of elastic scattering angular distribution with the weakly bound projectiles. A typical bi-parametric ΔE-E$_{res}$ spectrum for the ^{7}Li + ^{232}Th system at E$_{lab}$ = 44 MeV and θ_{lab} = 60° is plotted in Fig. 3.1, showing the isotopic separation of the reaction products. In the Fig. 3.2 we have plotted the projection on E$_{res}$ axis for the Z = 3 events, selected by using the banana gate. For angular distribution studies, the area of the peak of experimental data was acquired at different angles for every energies. The off line analysis of experimental data has been done by using the LAMPS software.

3.2 Data analysis of the elastic scattering angular distribution

3.2.1 Analysis using the Woods-Saxon potential

In the present analysis, the optical model fitting to the elastic scattering angular distribution data have been done using ECIS code [64]. The well known Woods-Saxon form of the interaction potential with only volume terms have been used for the purpose. In order to get the best fit for the experimental elastic scattering angular distribution optical model calculations have been done. In this calculation, three important optical parameters, namely, depth, radius and diffuseness were selected for both the real and imaginary part of the potential. Several sets of the above three parameters were selected to get the best fit. Finally, in order to avoid the fitting with too many variables, the real and imaginary radius parameters were fixed at 1.06 fm through out the analysis. This analysis procedure has been successfully adopted in the past by several groups [15, 18, 22, 23, 25, 27, 57]. Using this radius parameters, and varying the real and imaginary diffuseness optical potential parameters from 0.67 fm to 0.75 fm, was obtained the best fitting parameters for the elastic scattering angular distribution. In this analysis work, the best parameters values were acquired for diffuseness 0.71 fm. The real and imaginary radius and diffuseness parameters were fixed for all the bombarding energies. The real and imaginary of the depths optical potential parameters were varied to find the least value of χ^2 for both ^{6,7}Li + ^{232}Th reactions. The best fitting optical potential parameters and the total reaction cross sections are given in Tables 3.1 and 3.2 for ^{6,7}Li + ^{232}Th reactions respectively.

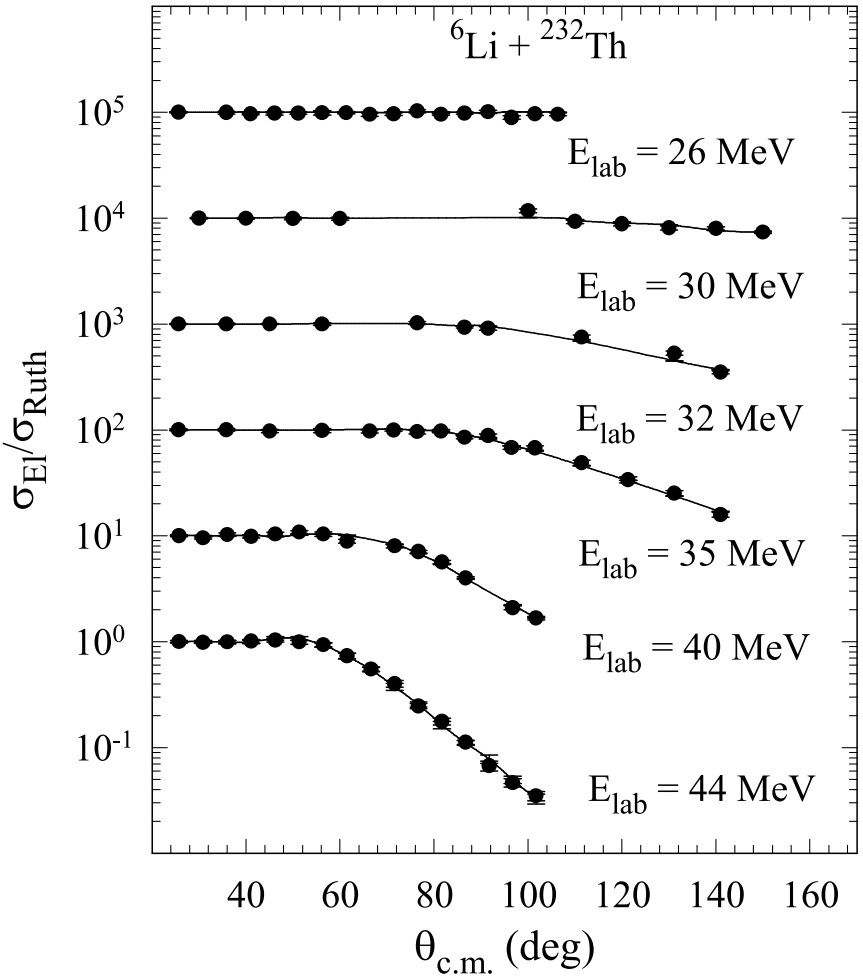

Figure 3.3: Experimental elastic scattering cross section (σ_{El}) normalized to the Rutherford cross section (σ_{Ruth}) as a function of $\theta_{c.m.}$ for the ^{6}Li + ^{232}Th system (solid circles) (suitably scaled up for each energy) and their best fits from optical model calculations (solid lines). The curves corresponding to the best fits by ECIS code.

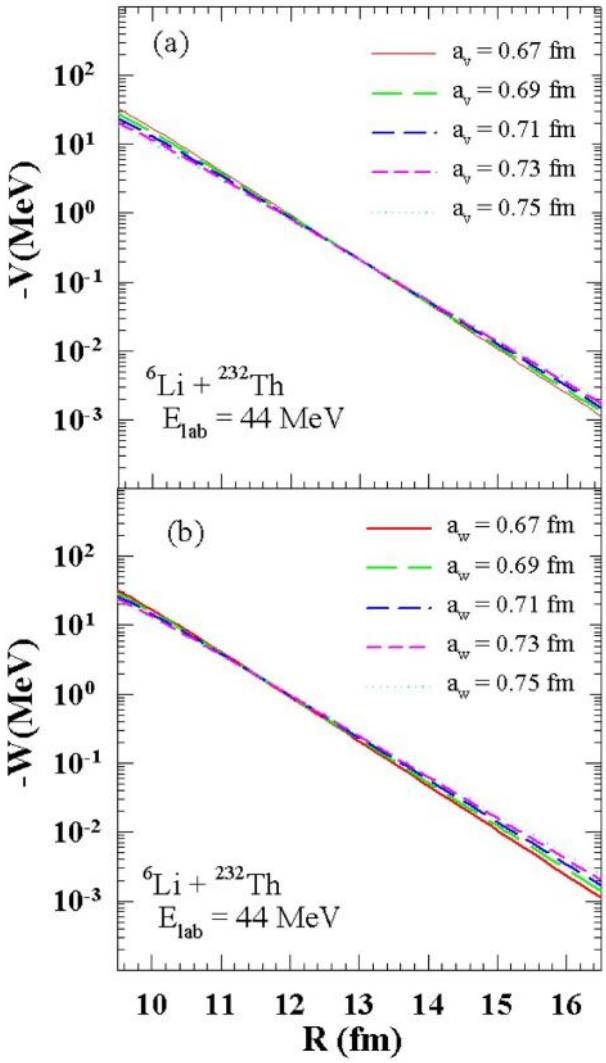

Figure 3.4: Figure of sensitivity of radius for 44 MeV for ^{6}Li + ^{232}Th systems, (a) real and (b) imaginary parts.

Table 3.1: Optical model parameters and total reaction cross sections for ^{6}Li + ^{232}Th system by ECIS code.

E_{lab} (MeV)	$r_o(fm)$	a_v & $a_w(fm)$	$V_r(MeV)$	$V_i(MeV)$	$\frac{\chi^2}{n}$	$\sigma_R(mb)$
26	1.06	0.71	105.6	90.00	2.33	3.884
30	1.06	0.71	263.3	167.7	1.70	105.4
32	1.06	0.71	215.9	394.6	2.37	404.4
35	1.06	0.71	130.2	183.5	1.02	561.2
40	1.06	0.71	97.69	136.0	2.39	970.6
44	1.06	0.71	128.8	144.7	0.68	1336

The best fitting parameters gives valuable information about energy dependence as shown in Table 3.1 and 3.2, which is a special indication of the elastic scattering. The results of the optical potential parameters from the analysis using WSP are shown in Figs. 3.3 and 3.5 for both ^{6,7}Li + ^{232}Th systems respectively. Several sets of optical potential shows good fit to the angular distribution on data. To decrease the opacities from the fitting of optical potential parameters, we have demarcated the radius of sensitivity for real and imaginary in two parts. For the observation of radius of sensitivity the parameters of radius were kept constant, real and imaginary part of depth, diffuseness parameters were varied for both systems. The intersection point have been recognized as a strong sensitivity radii [65], as observed for both the systems. Figs. 3.4 and 3.6 show the graph of sensitivity of radius for ^{6}Li + ^{232}Th and ^{7}Li + ^{232}Th systems respectively at one lab energy 44 MeV. The observation process of sensitivity of radius repeated for all bombarding energies and the average value was taken for both real and imaginary parts. Thus the average radius of sensitivity is 12.14 fm for ^{6}Li + ^{232}Th system and 11.27 fm for ^{7}Li + ^{232}Th system. The observation of sensitivity of radius is important for the study of dispersion relation. The radius and diffuseness parameters were kept constant for all the analysis work for both systems [15, 24, 27].

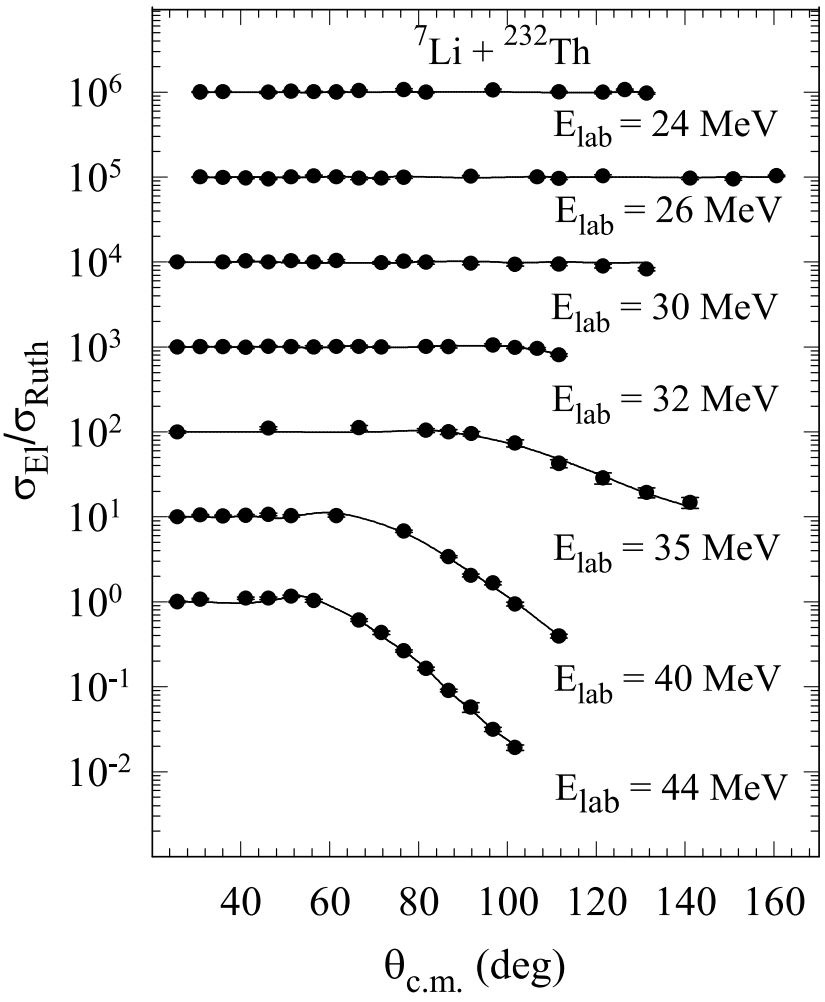

Figure 3.5: Experimental elastic scattering cross section (σ_{El}) normalized to the Rutherford cross section (σ_{Ruth}) as a function of $\theta_{c.m.}$ for the ^{7}Li + ^{232}Th system (solid circles) (suitably scaled up for each energy) and their best fits from optical model calculations (solid lines). The curves corresponding to the best fits by ECIS code.

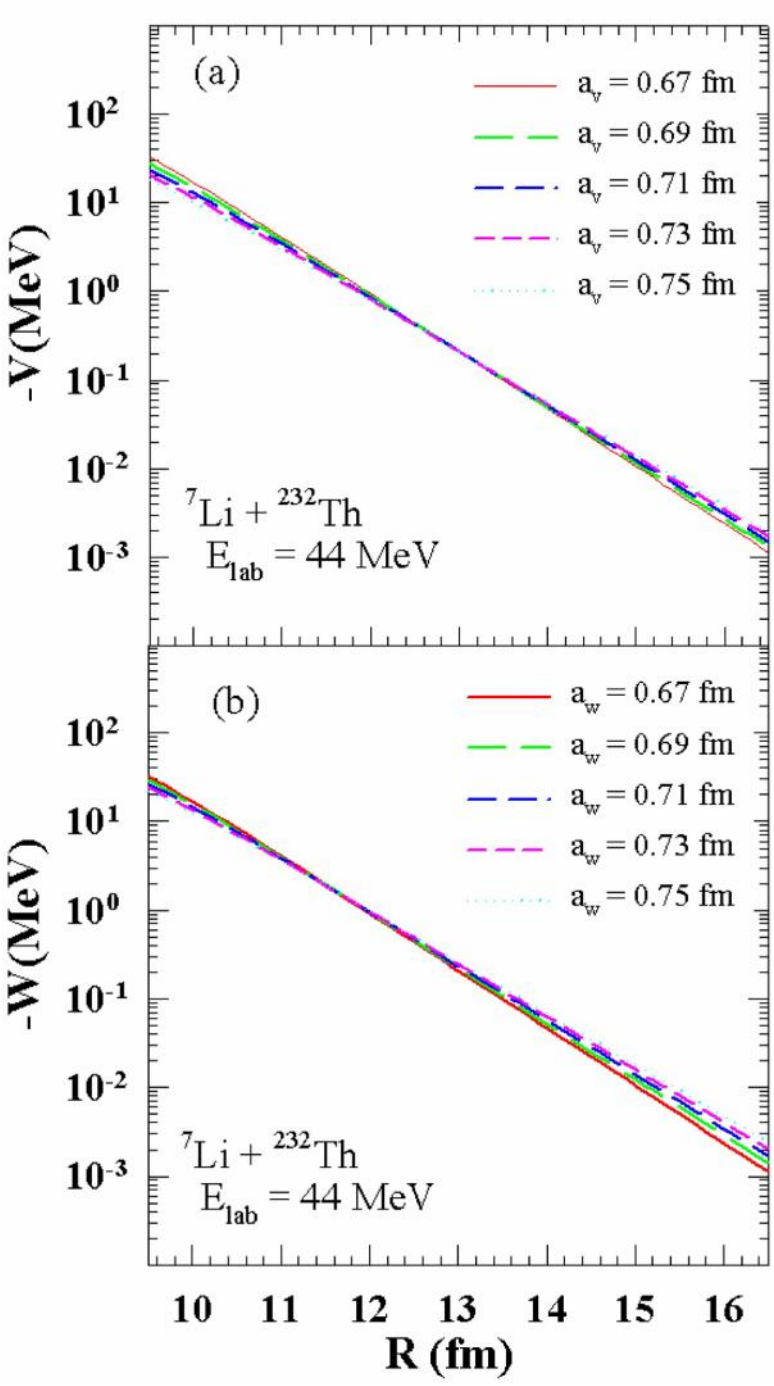

Figure 3.6: Sensitivity radius for ^{7}Li + ^{232}Th systems, (a) real and (b) imaginary parts at 44 MeV.

Table 3.2: Optical model parameters and total reaction cross sections data for ^{7}Li + ^{232}Th system by ECIS code.

E_{lab} (MeV)	$r_o(fm)$	a_v & $a_w(fm)$	$V_r(MeV)$	$V_i(MeV)$	$\frac{\chi^2}{n}$	$\sigma_R(mb)$
24	1.06	0.71	70.200	13.70	1.66	0.129
26	1.06	0.71	85.000	19.70	1.66	0.919
30	1.06	0.71	95.220	30.70	2.72	20.07
32	1.06	0.71	360.00	58.54	0.38	260.8
35	1.06	0.71	157.90	73.62	1.11	470.7
40	1.06	0.71	147.42	78.34	2.73	967.7
44	1.06	0.71	115.80	67.66	2.66	1215

3.2.2 Analysis using the double-folding Sao Paulo Potential (SPP)

The experimental elastic scattering angular distribution data have also been analyzed with Sao Paulo double-folding potential (SPP) [54, 55]. This potential have been formed on the basis of the Pauli non-locality principle. According to this principle, projectile and target exchange the nucleons. Through the SPP one can obtain fusion excitation functions, barrier distributions using the elastic scattering of weakly bound projectiles [66, 67].

In this present work, we have analyzed the elastic scattering angular distribution data for both ^{6,7}Li + ^{232}Th systems through Sao Paulo double-folding potential at given energies. The basic principle of double-folding potential is to make a comprehensive study of the nuclear densities obtained from experimental elastic scattering data. In this data fitting process only two normalization factors N_R and N_I for real and imaginary parts respectively.

Both the normalization coefficients N_R and N_I are energy dependent, thus they have the property of the dynamical polarization potential. These potentials are belonging to the dispersion relation. The figure of elastic scattering angular distribution

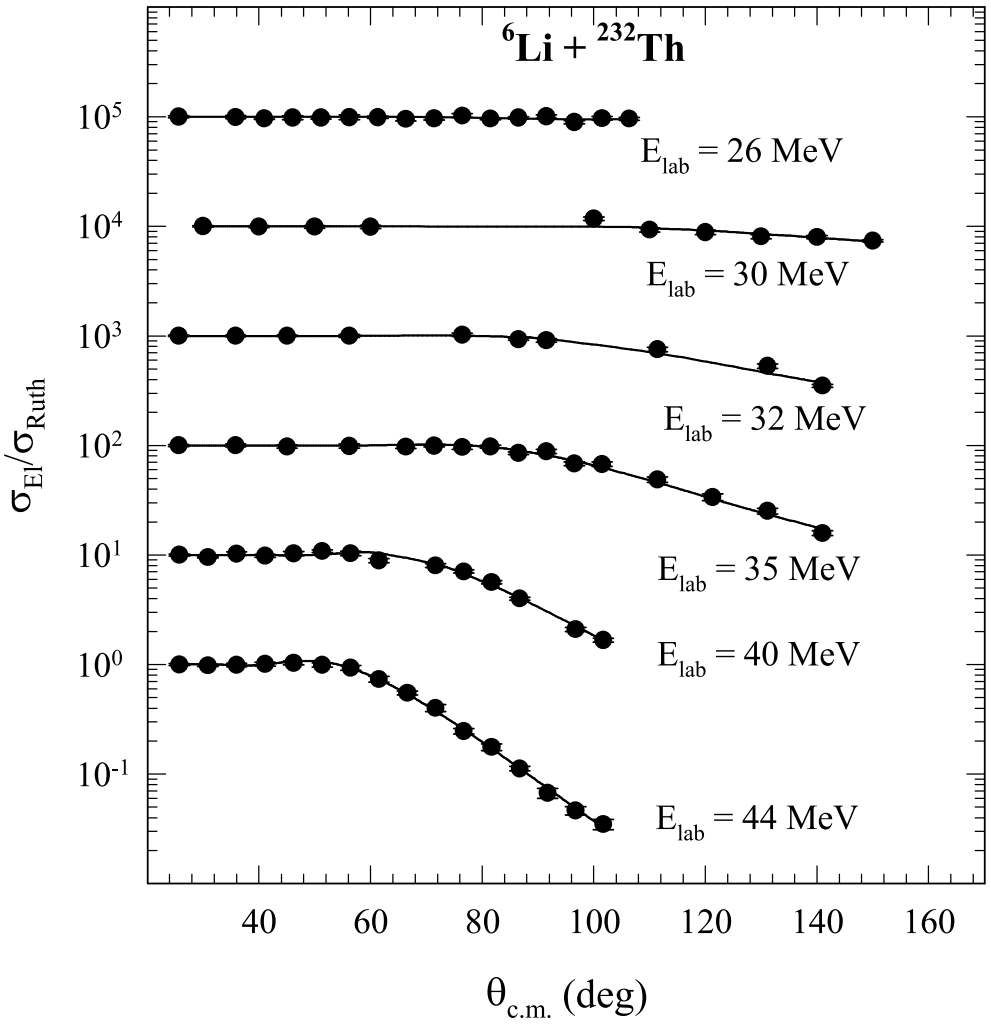

Figure 3.7: Elastic scattering angular distributions at different energies for the ^{6}Li + ^{232}Th system and their best fits from optical model calculations. The curves correspond to best fits were obtained using the Sao Paulo potential (SPP).

Table 3.3: Parameters and reaction cross sections obtained from the SPP calculations for the ^{6}Li + ^{232}Th system.

E_{lab} (MeV)	N_R	N_i	$\frac{\chi^2}{n}$	$\sigma_R(mb)$
26	0.72	1.06	1.92	3.57
30	1.41	1.72	2.08	107.0
32	1.29	3.68	2.64	398.4
35	0.82	1.52	1.45	550.6
40	0.87	1.09	2.71	963.6
44	0.80	1.24	0.51	1335

Table 3.4: Parameters and reaction cross sections obtained from the SPP calculations for the ^{7}Li + ^{232}Th system.

E_{lab} (MeV)	N_R	N_i	$\frac{\chi^2}{n}$	$\sigma_R(mb)$
24	0.81	0.36	1.66	0.114
26	0.94	0.45	1.57	0.807
30	1.55	0.55	2.01	18.90
32	2.00	0.56	0.36	260.6
35	0.88	0.61	1.19	471.9
40	0.83	0.60	2.82	959.7
44	0.66	0.53	2.89	1213

from the calculation of SPP is similar to the WSP calculations. The result of the normalization factors N_R and N_I are shown in Figs. 3.7 and 3.8. The best fit parameters and reaction cross sections data are presented in Tables 3.3 and 3.4 for ^{6,7}Li + ^{232}Th reactions respectively. From the observation of both the analysis, it may be concluded that the experimental elastic scattering data do not show model dependency. The optical potential parameters are consistence with the similar results as shown in (Fig.3.9) and (Fig.3.10).

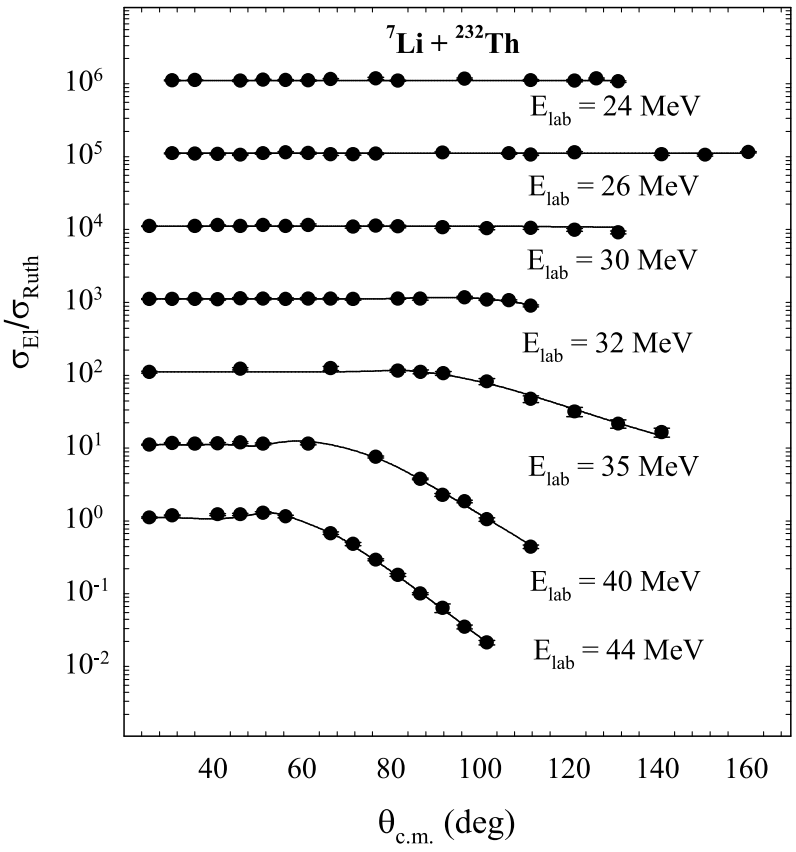

Figure 3.8: Elastic scattering angular distributions at different energies for the ^{7}Li + ^{232}Th system and their best fits from optical model calculations. The curves correspond to best fits were obtained using the Sao Paulo potential (SPP).

3.2.3 Dispersion Relation Analysis

For the understanding of the behavior of energy depended optical potential parameters, dispersion relation study is important [1, 13, 33, 68]. In the analysis of dispersion relation, the radius and diffuseness parameters are kept fixed and only the depth parameter is changed with the energy, so that it is acceptable for all the energies.

The details of this analysis given in the sec. (2.9) chapter 2.

$$\Delta V(E) = \frac{P}{\pi} \int_{-\infty}^{+\infty} \frac{W(E')}{E' - E} dE' \tag{3.1}$$

Equation 3.1 shows the relation between real and imaginary optical potential parameters. This equation has been used for the analysis of the dispersion relation.

In this analysis, the dispersion relation has been employed at the sensitivity of radius for all the bombarding energies. Three different sets of linear segment are applied on the imaginary potential for getting the real part. Fig. 3.9 shows the result of Woods Saxon potential analysis, where threshold anomaly has been presented in ^{7}Li + ^{232}Th reaction while breakup threshold anomaly in ^{6}Li + ^{232}Th reaction. Similar process is applied for Sao Paulo potential analysis and the result is shown in Fig. 3.10. The result from WSP and SPP shows similar behavior for both the systems. Earlier, there are several measurements reported for the study of dispersion relation through optical potential parameters [15, 21, 3, 22, 24, 27, 26, 25].

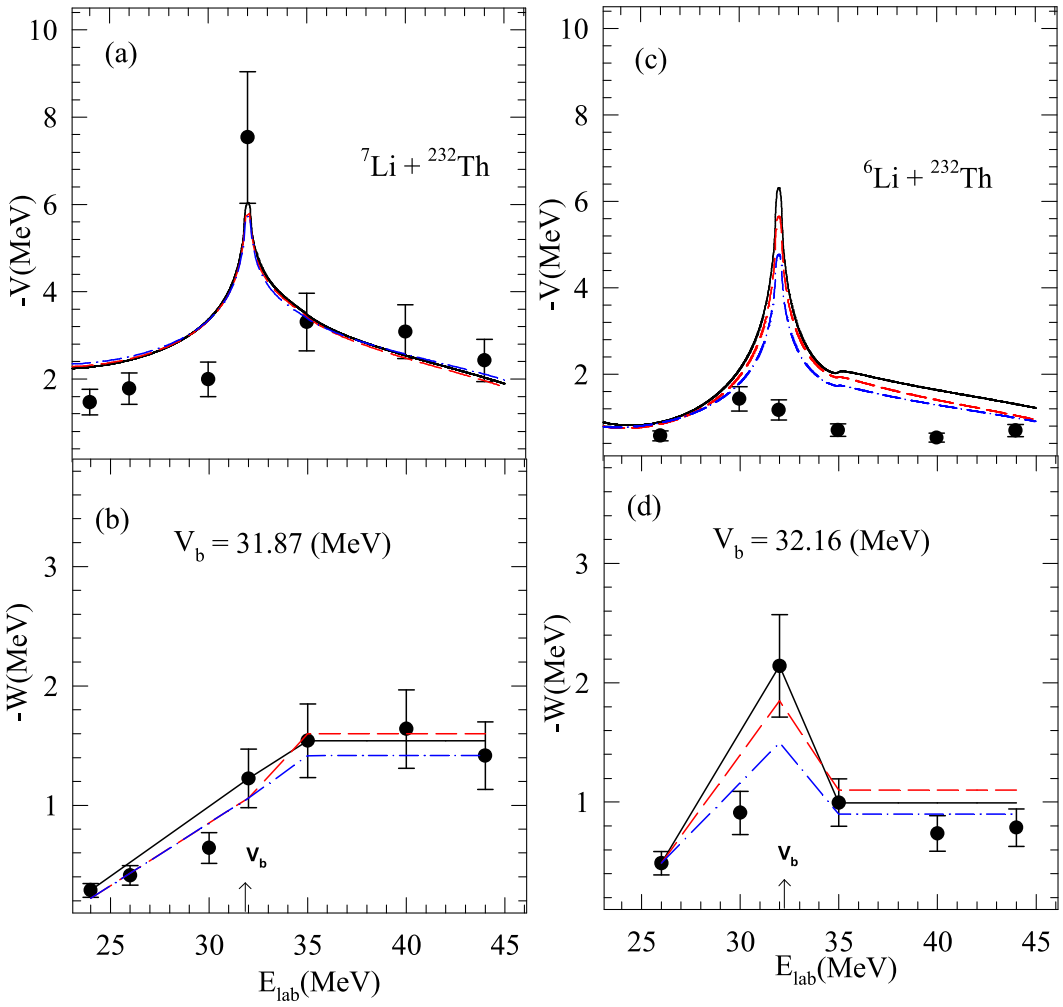

Figure 3.9: Energy dependence of the real and imaginary potentials at R_s = 12.14 fm and 11.27 fm for ^{6}Li + ^{232}Th and ^{7}Li + ^{232}Th systems, respectively. The straight line segments represent various fits of imaginary potential W(E) and the corresponding curves for real potential V(E) were obtained from these by using the dispersion relation. Figs. (a) and (b) correspond to the real and imaginary potential curves for ^{7}Li + ^{232}Th system, whereas (c) and (d) represent the ^{6}Li + ^{232}Th system.

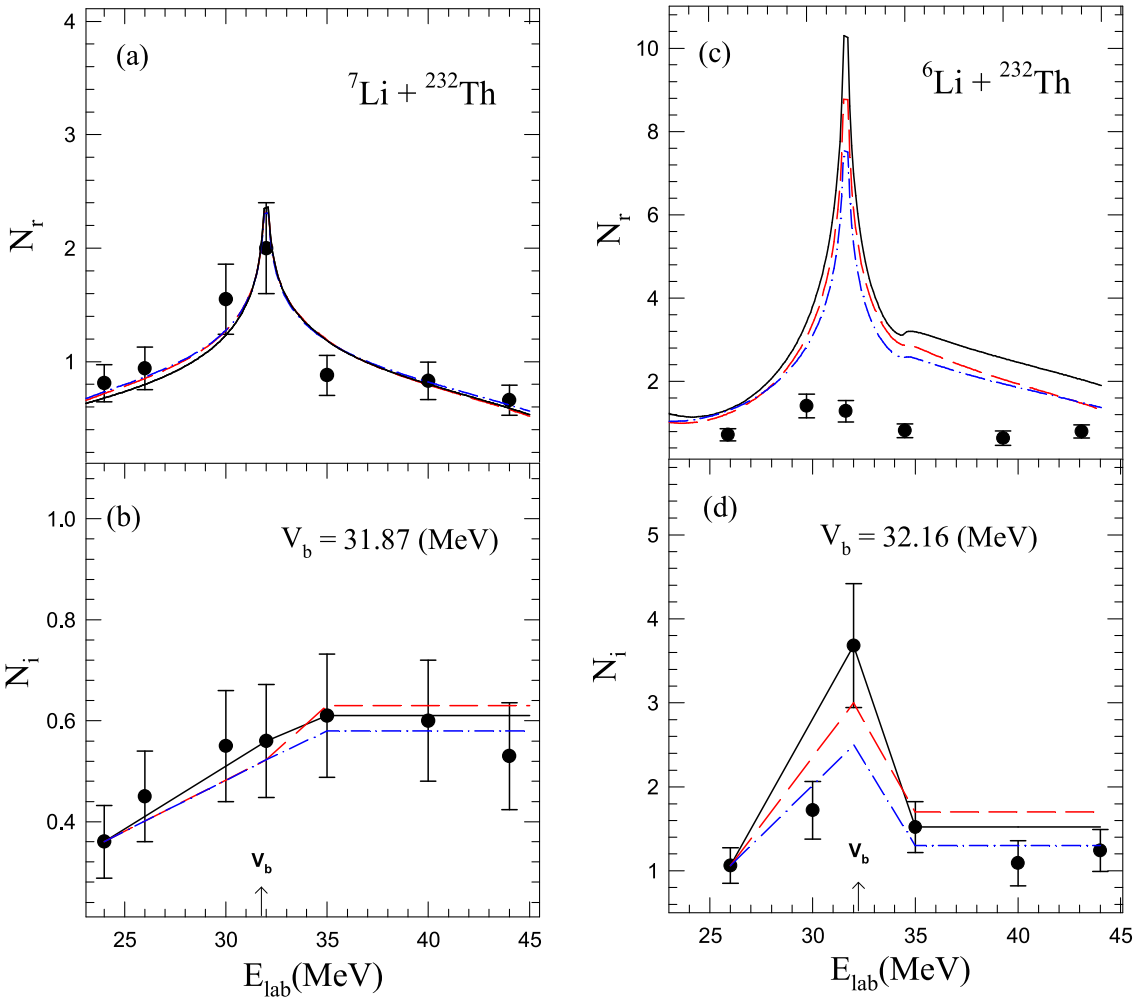

Figure 3.10: Energy dependence of the normalization factors N_R and N_I, for the real and imaginary potentials, corresponding to the Sao Paulo potential (SPP) with two free parameters, for the ^{6}Li + ^{232}Th and ^{7}Li + ^{232}Th systems. The lines represent possible behaviours of N_R and N_I that are compatible with the dispersion relation [7,14]. Figs. (a) and (b) correspond to the real and imaginary potential curves for ^{7}Li + ^{232}Th system, whereas (c) and (d) represent the ^{6}Li + ^{232}Th system.

3.3 Comparison of fission-fusion and total reaction cross section

The fusion cross sections for ^{6,7}Li + ^{232}Th systems have been calculated by using CCFULL code for all bombarding energies in step of 1 MeV [69]. In this calculation, the total reaction cross section have been obtained from the analysis of elastic scattering angular distribution data of ^{6,7}Li + ^{232}Th reactions and compared with the fusion-fission cross section [70]. Figs. 3.11(a),(b) and (c) show the comparison between total reaction and fusion-fission cross sections. The total reaction cross section was also calculated from elastic scattering angular distribution analysis for both systems. The reaction cross section of ^{6}Li has been found to be greater than ^{7}Li projectile. Similar behavior has been observed in the fusion and fission reaction cross section at sub barrier energies as shown in Figs. 3.11(b) and (c). This feature gives an indication that the breakup reaction cross section for ^{6}Li is more than that for ^{7}Li projectile. Similar measurements are also available in the literatures [71, 72].

The contribution of projectile fabrication in the coupling dynamics and the effect of breakup procedure in the fusion cross sections at around the Coulomb barrier energies, have been observed [73, 74, 75, 76]. In order to remove the size of projectile impact at reaction cross sections of ^{6,7}Li + ^{232}Th reactions, the "reduction" scheme was taken. This scheme introduced by Gomes et al. [77], has been successfully used in several systems [27, 78, 79]. Reduced reaction cross section values were obtained for both the systems at all the energies. In this procedure the quantities, for X axis is $E_{c.m.}$ $(A_P^{1/3} + A_T^{1/3})/Z_P Z_T$ and Y axis is $\sigma_R/$ $(A_P^{1/3} + A_T^{1/3})^2$.

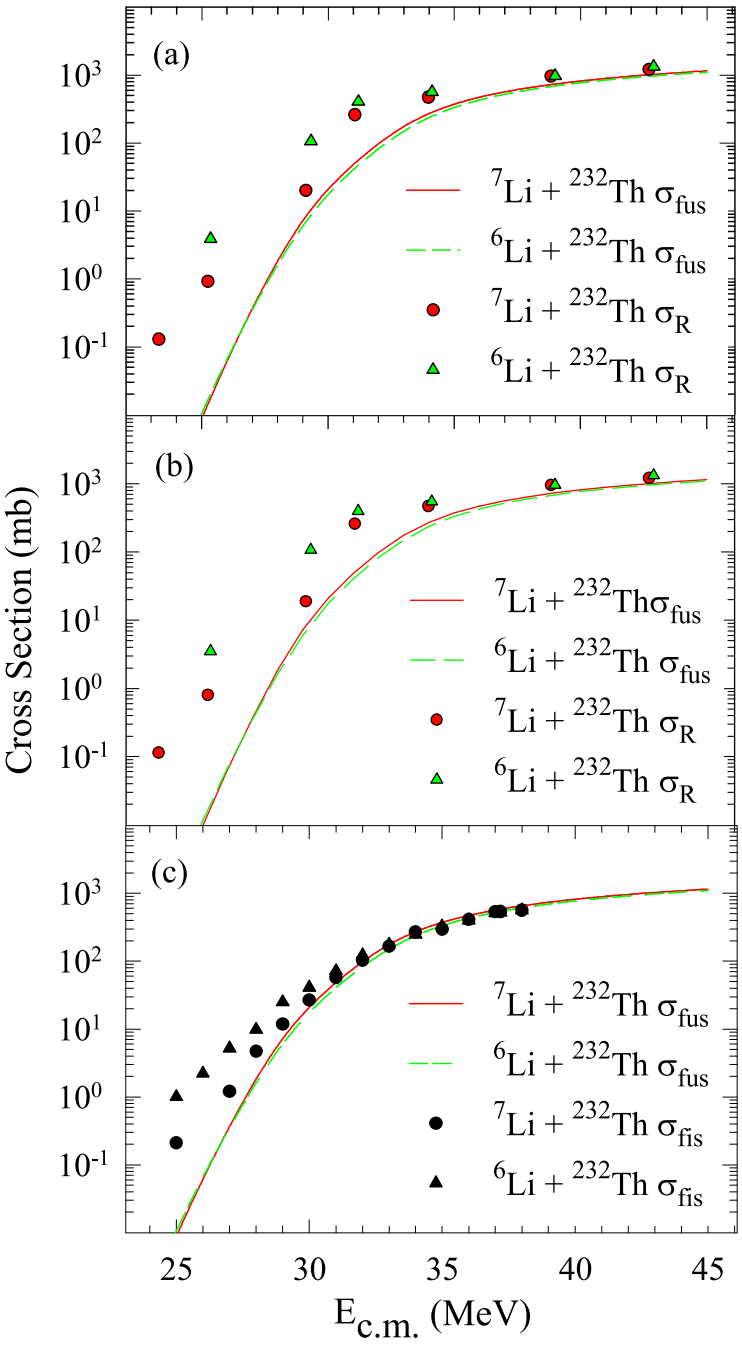

Figure 3.11: The total fusion cross sections (σ_{fus}) calculated by CCFULL and total reaction cross sections (σ_R) for the ^{6,7}Li + ^{232}Th systems obtained by using ECIS code and SPP calculation shown in 7 ((a,b)) respectively plotted as a function of the bombarding energy. The total fission cross sections (σ_{fis}) [60] and the total fusion cross sections for the ^{6,7}Li + ^{232}Th systems are plotted in 7 (c).

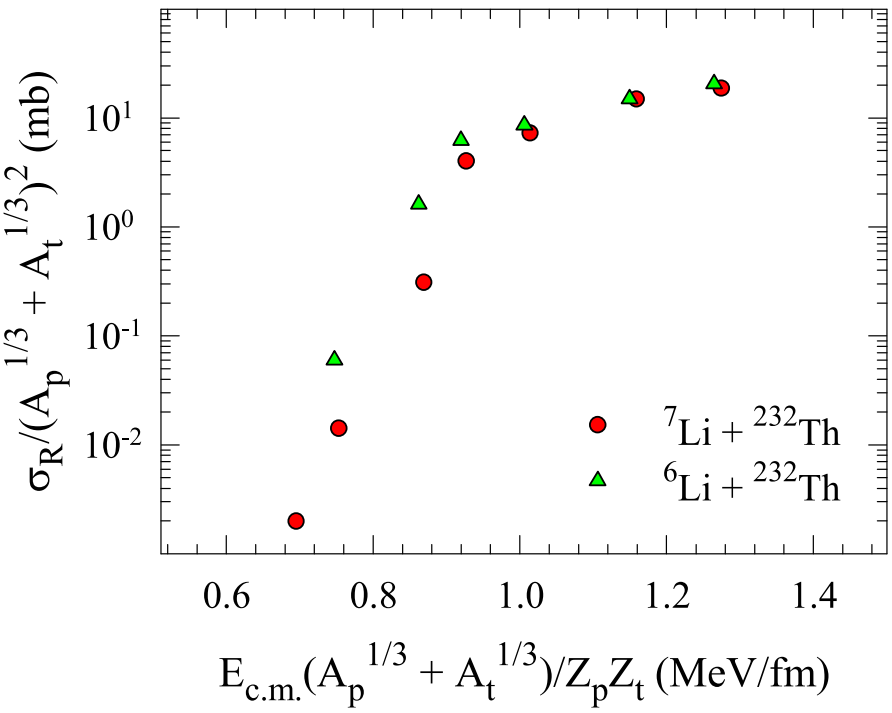

Figure 3.12: Reduced total reaction cross section vs reduced projectile energy for the ^{6,7}Li + ^{232}Th reactions using the prescription given in Ref [67].

In the above quantities, where $A_P^{1/3}$, Z_P and $A_T^{1/3}$, Z_T represent the mass and charge of projectile and target respectively, reaction cross section represented by σ_R. Fig. 3.12 shows the result of reduced total reaction cross sections for both systems. The reduced total reaction cross sections of ^{6}Li + ^{232}Th system is greater then ^{7}Li + ^{232}Th at sub barrier energies. This is one more sign of breakup inference in the ^{6}Li projectile [5, 20, 27].

3.4 Results and Discussion

The measurements of elastic scattering for ^{6,7}Li + ^{232}Th reactions at different bombarding energies around the Coulomb barrier have been done. For the analysis of experimental data we used Woods Saxon and Sao Paulo Potential. The results from the analysis have been compatible with the dispersion relation. The suitable parameters that allows best fit of the angular distribution data were acquired from the mechanism of χ^2-minimization. The threshold anomaly has been observed for ^{7}Li + ^{232}Th reaction and breakup threshold anomaly for ^{6}Li + ^{232}Th reaction. Other important result is that the reaction cross section of ^{6}Li + ^{232}Th reaction is larger than ^{7}Li + ^{232}Th reaction at below barrier energies.